RSC Advances

PAPER

View Article Online
View Journal | View Issue

Cite this: *RSC Adv.*, 2017, **7**, 21600

Laser-textured surface storing a carbon dots/poly(ethylene glycol)/chitosan gel with slow-release lubrication effect†

Hailin Lu,[a] Shanshan Ren,[a] Pengpeng Zhang,[a] Junde Guo,[a] Jianhui Li*[b] and Guangneng Dong*[a]

Received 26th February 2017
Accepted 5th April 2017

DOI: 10.1039/c7ra02387a

rsc.li/rsc-advances

Arthroplasty presents wear problems because body fluid, as the only lubricant, has poor performance. However, normal lubricants become diluted by body fluid and then are absorbed by the human body. To prolong the lubricant's effectiveness, this study prepared a carbon dots/poly(ethylene glycol)/chitosan (CDs/PEG/CS) composite gel, which, stored in laser textures, could slowly release the lubricant. Laser-textured surfaces can simultaneously store CDs/PEG/CS gel and wear debris. In this study, CDs, PEG and chitosan (CS), which have biocompatibility and biodegradability properties, can be used in the human body. CDs/PEG/CS gel was added to the laser textures and had excellent slow-release properties, which became better under pressure. Meanwhile, carbon dots (CDs) associated with poly(ethylene glycol) (PEG) *via* hydrogen bond formed an excellent lubricant, which led to the good lubrication effect. This study provides a new and green approach to enhance the tribological performance of artificial joints.

1. Introduction

Arthroplasty increases the wellbeing of patients. More and more people look forward to the long-term service life of artificial joints. The joint capsule is removed after joint replacement surgery, and the body fluid becomes the only lubricant, but it has poor lubrication effect.[1] Ultra-high molecular weight polyethylene (UHMWPE) has been used successfully as a bearing material in orthopaedic total joint replacements for decades.[2] The most popularly used bearing couple for artificial joint systems is the combination of UHMWPE acetabular component and a metal femoral component.[3] However, wear particles are produced by the wear of UHMWPE, and osteolysis is triggered by inflammatory responses to UHMWPE wear particles.[4–6] As a result, more wear debris is generated due to the poor lubrication of body fluid, and the service life of artificial joints are seriously shortened,[7] thus the patient will suffer more infection risks and pain from frequent injections. Prosthetic joints release excessive microscopic wear debris into the joint space under the poor lubrication effect, and then the bones face inflammation and osteolysis. Wear debris is the primary reason of the aseptic loosening phenomenon in artificial joint replacement.[8–11]

However, many different strategies and techniques have been introduced to reduce the number of UHMWPE wear particles and extend the longevity of artificial joints.[12–15] But those technologies could not enhance the lubrication effect efficiently. In this study, a carbon dots/chitosan/poly(ethylene glycol) (CDs/CS/PEG) composite was made to reduce the friction coefficient. Chitosan (CS) and poly(ethylene glycol) (PEG) have good biodegradability and biocompatibility properties,[16–20] and PEG has been frequently used for lubrication.[21] Carbon dots (CDs), which are discrete quasi-spherical nanoparticles with sizes less than 10 nm, exhibit dependence of photoluminescence (PL) on size and excitation wavelength.[22] Xu *et al.* first reported CDs and fluorescent carbon nanoparticles in 2004.[23] Wang *et al.* used ionic liquid carbon dots as a high-performance friction-reducing and anti-wear additive for PEG.[24] Huang *et al.* used carbon quantum dot/CuS_x nanocomposites towards highly efficient lubrication and metal wear repair.[25] CDs have many virtues compared with traditional quantum dots, such as abundant precursors, excellent solubility in various kinds of solvents, preferable biocompatibility, and exceptional resistance to photobleaching.[26] CDs, PEG and CS have a lot of hydroxyl and epoxy groups on their surfaces. Thus, they associate with each other *via* hydrogen bond and may form a particular structure in solution.

Good lubrication is very important to artificial joints. In animals, cartilage joints have a friction coefficient in the range of 0.001–0.03 when the pressure between the bone surfaces reaches as high as 3–18 MPa.[27,28] This study prepared CDs/PEG/CS composite that could effectively protect the surfaces of UHMWPE and thus prolong the service life of artificial joints.

[a]*Key Laboratory of Education Ministry for Modern Design and Rotor-Bearing System, Xi'an Jiaotong University, Xi'an 710049, China. E-mail: donggn@mail.xjtu.edu.cn; 6626640@qq.com; Fax: +86 029 83237910; Tel: +86 029 82668552*

[b]*Department of Chemistry, School of Science, Xi'an Jiaotong University, Xi'an 710049, China. E-mail: 840780812@qq.com*

† Electronic supplementary information (ESI) available. See DOI: 10.1039/c7ra02387a

Because CS is a crystalline polysaccharide, there are strong intramolecular and intermolecular hydrogen bonding interactions in the structure. Thus, CS cannot be dissolved in distilled water, and auxiliary acetic acid solution is used to dissolve CS.[29] In this study, 1 wt% NaOH solution was used to solidify the CDs/PEG/CS sol. NaOH could neutralize acetic acid in CDs/PEG/CS, decreasing the solubility of CS and re-forming the hydrogen bonding network.[29] As a result, the gel formed by the NaOH treatment method could prevent the CDs/PEG/CS composite from dispersing outside of a laser-textured surface, and the textures also can store wear debris; this slow-release solution has excellent lubrication effect. This technology prepared an excellent lubricant *via* a simple method, and this CDs/PEG/CS composite material can effectively protect the surfaces of UHMWPE and thus prolong the service life of artificial joints efficiently.

2. Experimental

2.1 Materials

Poly(ethylene glycol) (PEG, molecular weight, 4000) was from Guangdong Guanghua Sci-Tech Co., Ltd. (Guangdong, China). Chitosan (CS, degree of deacetylation ≥ 90%; molecular weight, 700–800 kDa) was from Shanghai Lanji Technology Co., Ltd. (Shanghai, China). All the materials used in the research were analytical-reagent grade (AR).

2.2 Preparation

Synthesis of nitrogen-doped carbon dots:[30–32] 1.2 g of DL-alanine and 30 mL of deionized water was added to a 100 mL beaker. The mixture was stirred for 30 min at room temperature to yield a clear solution. The clear solution was then added to the reaction vessel of the microwave reactor. Five minutes were required to increase the temperature of the reaction vessel up to 200 °C. The reaction vessel was maintained at 200 °C for 60 min by microwave irradiation and then cooled to room temperature. The transparent aqueous solution was subjected to dialysis (M_w = 1000) for 7 days to eliminate the excess residue.

The CDs, PEG and CS were mixed in a bottle, and 1 wt% acetic acid solution was added. The mixture was stirred at 500 rpm for 1 h to obtain a homogeneous CDs/PEG/CS solution. The CDs/PEG/CS sol was added to 1 wt% NaOH solution to form CDs/PEG/CS gel, which was then washed until neutral by distilled water. The gel was placed in ethanol solution for 12 h, then dried in an oven for 24 h at 30 °C. The dry CDs/PEG/CS composite was placed in distilled water for 1.5 h to form a gel; this gel, containing 75.6 wt% water, was prepared for tribology tests.

Laser technology was used to manufacture surface texture on Co–Cr–Mo alloy surfaces.[33,34] The rounded textures were 100 μm diameter, 85 μm depth and 200 μm spacing.

2.3 Friction tests

The tribological properties were investigated using a ball-on-disc tribometer (UMT-2, CETR Corporation Ltd, USA) in a reciprocating friction drive system. Experiments were performed at room temperature (25 °C). All tests were repeated five times, and the average was taken. The disk was CoCrMo alloy (*Φ*30 mm, surface roughness 0.017 μm), and the ball was UHMWPE (*Φ*9.5 mm, surface roughness 18 μm). The samples were slid against the disk with a load of 5 N (10.9 MPa) for 15 min at the sliding speed of 24 mm s^{-1}.

2.4 Characterization

A diode slide-pump laser (QC-F20, Xi'an Qingchuang) was used to manufacture surface textures on Co–Cr–Mo surfaces. The worn surface microstructure was observed by surface profiler (TR-200, Time Group). FT-IR infrared analysis was carried out between 400 and 4000 cm^{-1} using a Bruker spectrophotometer (TENSOR27, Bruker, Germany). All measurements were carried out with 64 scans at a resolution of 0.16 cm^{-1} at room temperature. XRD was carried out using a D8 (D 76181 Karlsruhe, Bruker AXS, Germany) X-ray diffractometer with Cu Ka radiation (λ = 0.15406 nm), running at 40 kV and 40 mA, and scanning from 10° to 90°. Transmission electron microscope (TEM) (G2F30, FEI, USA) was used to observe the morphology of the CDs. XPS (AXIS Ultrabld, Kratos, England) was used to analyse the CDs. Fluorescence analysis (QuantaMaster400, PTI, USA) was used to observe emission wavelength shift from 250 nm to 600 nm when the excitation wavelength was increased from 390 nm to 430 nm. The surface micro-topography and surface profile curve were measured using a 3D confocal microscope (OLS4000, OLYMPUS Company, Japan).

3. Results and discussion

3.1 TEM and fluorescence analysis of CDs

In this work, the CD morphology images were evaluated by TEM, as shown in Fig. 1. The as-prepared CDs dispersed uniformly. The particles have different sizes, and most of them were 18 nm. Emission wavelength shifted from 250 nm to 600 nm when the excitation wavelength increased from 390 nm to 430 nm, with the strongest emission intensity at 465 nm (Fig. S1†). This phenomenon could be due to the emissions from different-sized CDs.[35,36]

3.2 XPS analysis of CDs

XPS characterization was used to analyse the composition of elements and their chemical state. The atoms of C, N, and O in

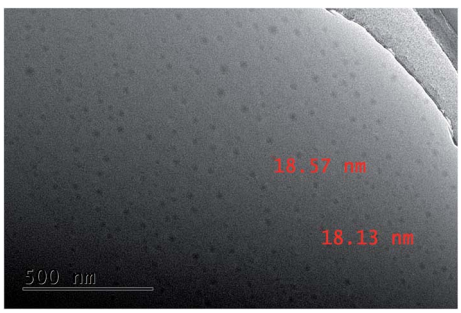

Fig. 1 The TEM image of CDs.

CDs were detected at the peaks of *ca.* 283 eV, 399 eV, and 531 eV, respectively, as shown in Fig. 2a. Fig. 2b–d shows the high-resolution XPS for O 1s, N 1s and C 1s. As shown in the O 1s spectrum, O atoms mainly presented in two groups: C=O at 530.5 eV and C–OH at 531.9 eV.[37] N 1s spectrum could be divided into two main peaks: 398.5 eV for pyridinic N and 399.3 eV for lactam and imide N.[38] For the C 1s spectrum, distinct peaks at 283.3 eV, 284.5 eV and 287.3 eV were attributed to the bonds of graphite-like sp^2 C, C=N and C–N (overlapped with C=O), respectively.[39–41]

3.3 FT-IR and XRD analysis

Fig. 3a and S2† shows the absorption band at 3434 cm^{-1} indicating the terminal hydroxyl group, the brand at 2882 cm^{-1} due to the C–H stretch of CH_2, and the absorption band at 1108 cm^{-1} attributed to the C–O–C functional group.[42,43] CS, PEG and CDs have the same absorption peaks at 3434, 2882 and 1108 cm^{-1} because they have the same functional groups. The adsorptions at 961 and 842 cm^{-1} are attributed to the crystal band and the C–C–O bonds in PEG.[43,44] The band at 1591 cm^{-1} is attributed to C=C in CDs.[45] In the above peaks, PEG and CDs/PEG/CS curves depicted a similar behaviour at a particular frequency band. Fig. 3b shows the XRD patterns of CDs, PEG, CS and CDs/PEG/CS. The crystalline PEG powder shows intensive X-ray pattern, in accordance with previous studies.[46–48] The diffraction peaks at about $2\theta = 20.1°$ are attributed to the diffraction of the CS matrix.[29,49] The XRD spectrum of the CDs/PEG/CS material also had two peaks at 19.3° and 23.5°, which

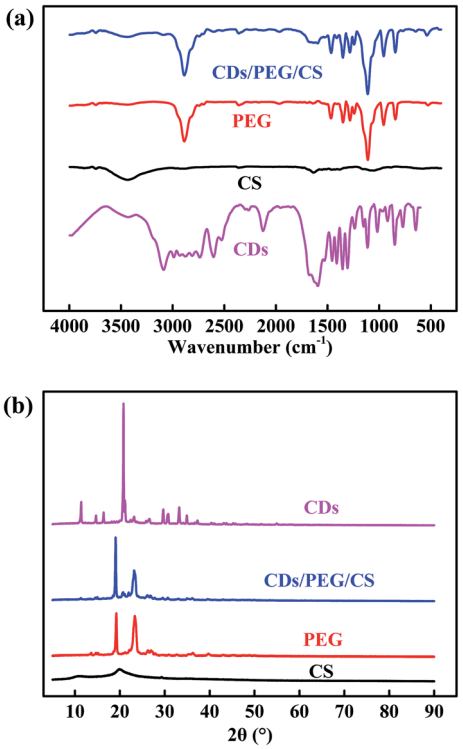

Fig. 3 (a) The FT-IR spectra and (b) XRD patterns of CDs, PEG, CS and CDs/PEG/CS (5 wt%/30 wt%/2 wt%).

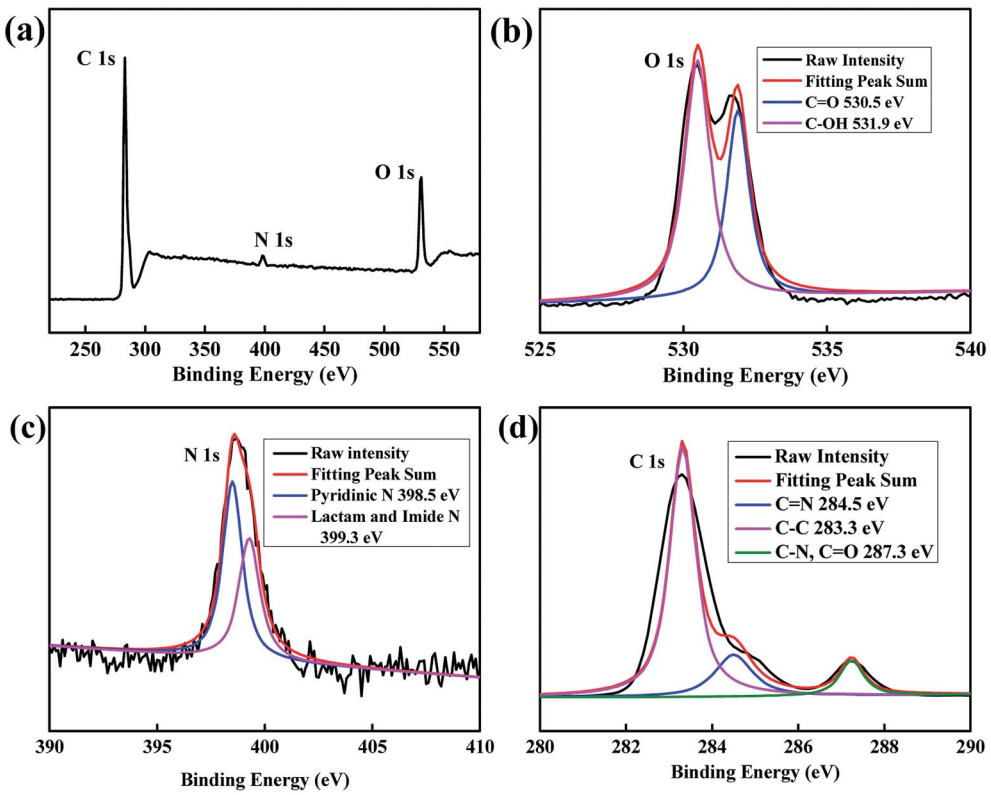

Fig. 2 (a) The XPS spectra of CDs, (b) the high resolution XPS of O 1s, (c) the high resolution XPS of N 1s and (d) the high resolution XPS of C 1s.

were located at the same position as the PEG powder, but the two peaks were of different intensities. As shown in Fig. 3b, the XRD pattern of CDs gives a sharp peak at 20.8°, which indicates densely packed alkyl groups.[26,50] Taken together, the FT-IR and XRD data demonstrate that CDs and CS mixed with PEG did not undergo any compositional/functional group changes.

3.4 The lubrication effect of different materials

Different materials have different lubrication effects. It is obvious in Fig. 4 that distilled water, 5 wt% CDs, 2 wt% CS, CDs/PEG/CS (5 wt%/30 wt%/2 wt%) and 30 wt% PEG have high average friction coefficients; they achieved 0.061, 0.042, 0.039, 0.023 and 0.016, respectively. Fig. S3† shows the average friction coefficient of CDs/PEG/CS sol under the load of 3–10 N (9.2–13.7 MPa). It has the highest average friction coefficient at 3 N, and the lowest average friction coefficient after 5 N; these data are relatively stable. In summary, this evidence proved that CDs/PEG/CS sol had good lubrication effect under high pressure. The average friction coefficient of CDs/PEG sol (5 wt%/30 wt%) achieved was 0.009, obviously better than the other materials in Fig. 4. Because the CDs/PEG solution has excellent lubrication effect, the CDs/PEG/CS gel slow-release solution may have good lubrication effect when this gel releases CDs and PEG.

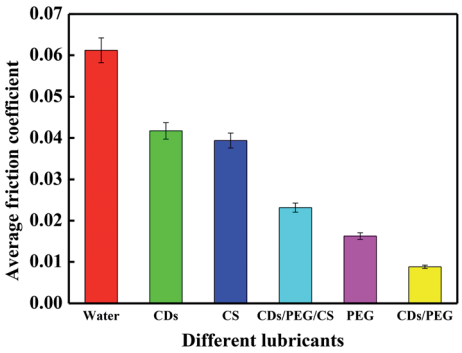

Fig. 4 Average friction coefficient of distilled water, 5 wt% CDs, 2 wt% CS, CDs/PEG/CS (5 wt%/30 wt%/2 wt%), 30 wt% PEG and CDs/PEG (5 wt%/30 wt%).

3.5 The friction coefficient of CDs/PEG/CS on textured surfaces

Laser surface texturing technology was used to manufacture surface texture on Cr–Co–Mo alloy surfaces. Lasers have been widely used for submicron processing and the ability to work in air because of their unique advantages of being a non-contact process and capability to generate complicated structures without the need for photo masking. The parameters of laser surface texturing are shown in Fig. 5: 100 μm diameter, 85 μm depth and 200 μm spacing. A principal application of dimples is the retention of lubricant and trapping of wear debris, which significantly reduce the tendency of galling and scoring in the hip joint movement.

Artificial joints are surrounded by lubricants with excellent lubrication effect. However, most lubricants are diluted by body fluid and absorbed by the human body, and this shortage affects the service life of artificial joints. In this research, the shortcomings are solved; the CDs/PEG/CS sol transforms to gel when 1 wt% NaOH solution is added. The CDs/PEG/CS gel in the textures of artificial joints can slowly release CDs and PEG, and wear debris is then stored in the textures. The CDs/PEG/CS gel stored in laser textures solves the problem that CDs/PEG/CS sol is easily consumed. The CS/PEG gel in the texture of the

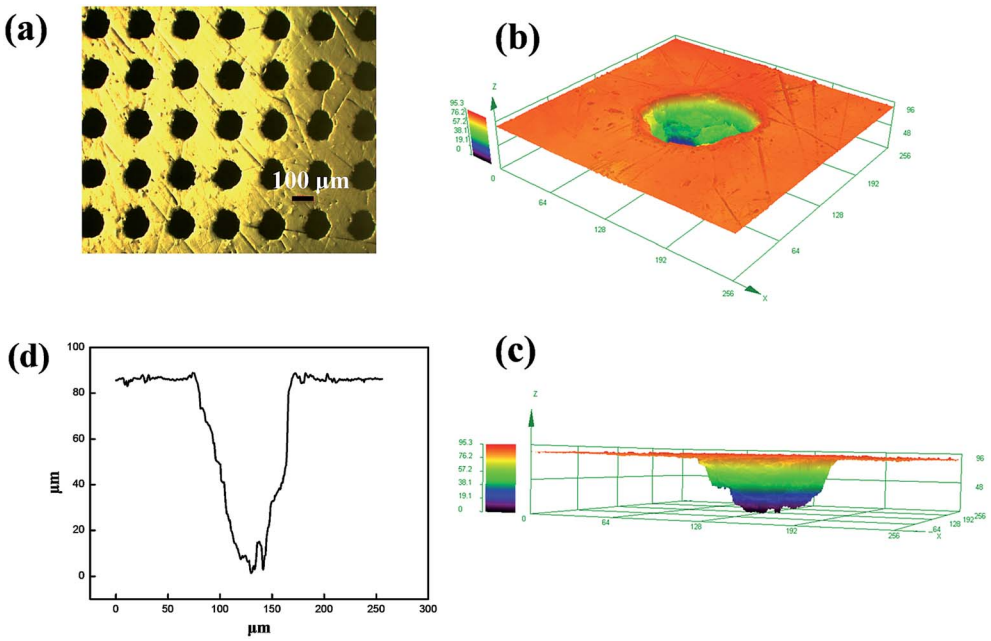

Fig. 5 Laser textures on Co–Cr–Mo surfaces: (a) the surface morphology of the texture, (b) the 3D surface morphology of the texture, (c) the 3D inner profile of the texture and, (d) the profile curve of the texture.

artificial joint is extruded under the movement by UHMWPE joints, then the CDs and PEG flow into the friction interfaces, causing excellent lubrication effect. But the composite loses water *via* evaporation with time, which caused the friction coefficient increase with the time, as Fig. 6 shows.

(CDs/PEG/CS) sol test: CDs/PEG/CS sol was added on the disk for the friction tests. (CDs/PEG/CS) gel test: CDs/PEG/CS sol was added on the disk to form CDs/PEG/CS gel by adding 1 wt% NaOH solution, washed until neutral by distilled water, then the disk was placed in ethanol solution for 12 h and washed three times by distilled water. It was found in Fig. S4† that the average friction coefficients of CDs/PEG/CS sol were 0.026 and 0.021 on textured surfaces and smooth surfaces, respectively. That of the CDs/PEG/CS gel reached 0.030 and 0.023 on textured surfaces and smooth surfaces, respectively. In summary, the CDs/PEG/CS gel has relatively higher friction coefficient than CDs/PEG/CS sol, but the CDs/PEG/CS sol will be diluted by body fluid and absorbed by the human body. The textures can store the CDs/PEG/CS gel and slowly release the CDs/PEG lubricant, thus causing good and long-lasting lubrication effect. So, the next step is to test the slow-release effect of CDs/PEG/CS gel.

3.6 The effect of slow release and release under pressure

CDs/PEG/CS gel release properties affect the lubrication effect. In this study, 0.15 g dry CDs/PEG/CS composite was added to 3.0 g distilled water, and the tribology properties of the releasing solution were tested, with the PEG/CS composite tested under the same conditions. The results are shown in Fig. 7. Fluorescent spectrum was used to detect CDs. Fig. S5† revealed that the release solution contained CDs. The CDs/PEG/CS gel slow-release solution had better lubrication effect than PEG/CS gel, showing that the CDs/PEG/CS gel-released CDs and PEG had better lubrication effect. The release process was slow; the lubrication effect of the release solution did not achieve stability after 9 days of release.

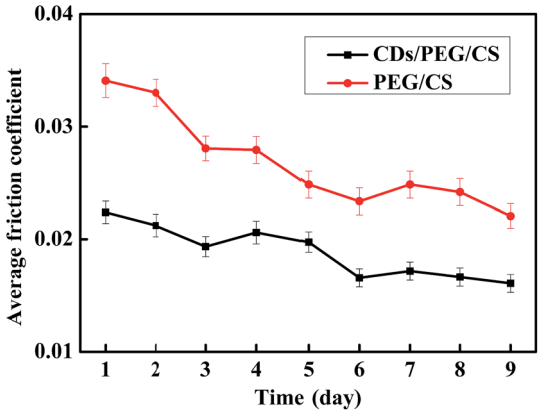

Fig. 7 Standing release for different days.

Measuring only the standing releasing effect is insufficient to determine the gel's application in artificial joints; this CDs/PEG/CS gel may be extruded in the human body. Thus, a centrifugal machine was used to simulate the extrusion pressure with different rotation speeds to calculate the release effect. In this experiment, 0.15 g dry CDs/PEG/CS composite was immersed in 3 g distilled water for 1.5 h. These samples were centrifuged at the rotation speed of 500–4000 for 10 minutes; PEG/CS

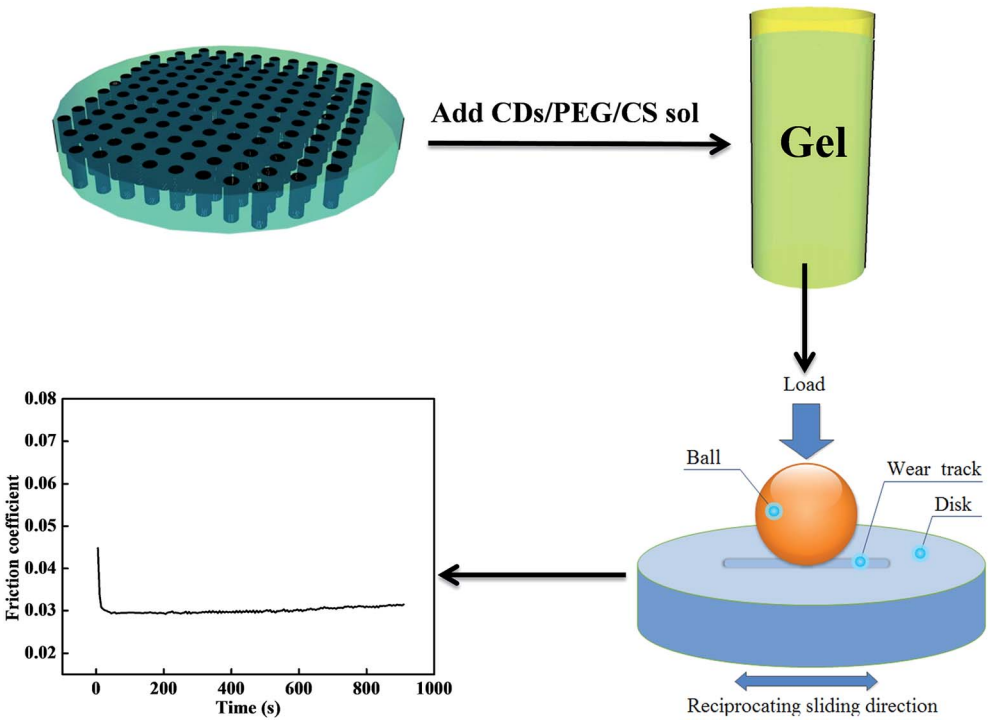

Fig. 6 The friction tests on textured surfaces.

composite was tested under the same condition. The pressure increased with the rotation speed increase, as Fig. 8 shows. This reveals that the composite gel released more lubricant under high rotation speed, and the CDs/PEG/CS gel released solution had better lubrication effect than the PEG/CS gel released solution. In conclusion, these data reveal that these gels released slowly on normal condition, but are released faster under the conditions of strenuous exercise because of high pressure.

3.7 Worn surfaces of Co–Cr–Mo disk and UHMWPE ball

The worn surfaces are a very important sign in tribology. In this study, the UHMWPE ball underwent reciprocating sliding for 2 h on the surfaces of Co–Cr–Mo disks. Fig. S6† shows the original surfaces of the UHMWPE ball; there are regular scratches from machining. Fig. 9a shows tiny wear traces, the worn surfaces on the original morphology when using slow-release solution as lubricant, with only some minor scratches on the worn surface. But there are obviously wear characteristics in Fig. 9b; the UHMWPE ball surface presents serious wear condition. The Co–Cr–Mo has good anti-wear property. Fig. 9c presents the wear on the original morphology; the surfaces were smooth when slow-release solution was used as lubricant. But in Fig. 9d, the surfaces of Co–Cr–Mo disk sliding under distilled water presented plough wear characteristic after 2 h friction. These worn surface figures proved that the slow-release solution had excellent lubrication effect and effectively reduced the wear condition.

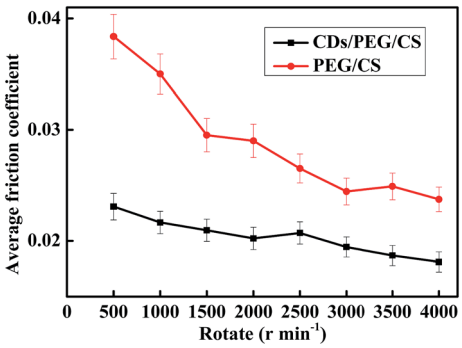

Fig. 8 Release by centrifuge under different rotation speeds.

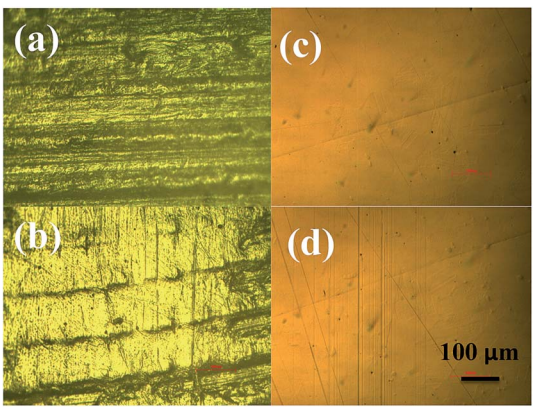

Fig. 9 Worn surfaces of UHMWPE ball after 2 h friction: (a) with slow-release solution (CDs/PEG/CS 3 days) and (b) with distilled water; worn surfaces of Co–Cr–Mo disk after 2 h friction (c) with slow-release solution (CDs/PEG/CS 3 days) and (d) with distilled water.

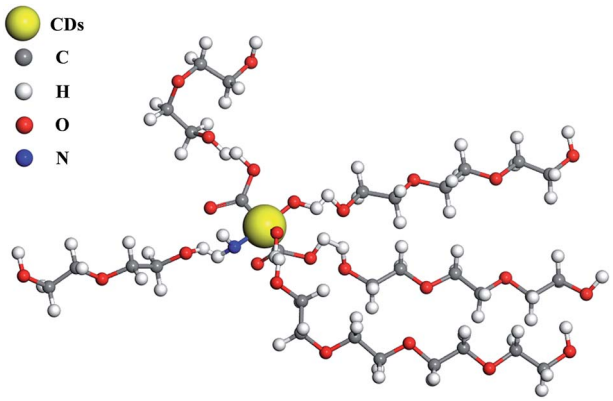

Fig. 10 CDs associate with PEG to form a particular structure.

3.8 Relevant mechanisms

There are amidogen ($-NH_2$), hydroxyl (–OH) and carboxyl (–COOH) groups on CDs (Fig. 2), and the PEG chain also has hydroxyl group; thus, they will associate with each other to form a particular structure *via* hydrogen bonds, as Fig. 10 shows. PEG has good lubrication effect in low concentration, as Fig. S7† shows. It is obvious that the average friction coefficient decreased with the concentration increasing from 0.035 to 0.025, corresponding to the PEG concentration of 0.5–5 wt%. But in slow-release experiments (Fig. 7 and 8), 0.15 g dry composite was added in 3 g distilled water, and the mixed materials contained 95.2% water. Thus, the slow-release solution contained less than 5 wt% PEG, but most of the average friction coefficients were below 0.02 when CDs were added, as Fig. 7 and 8 show. These above data reveal that CDs' association with PEG *via* hydrogen bond effect may be the primary factor causing the good lubrication effect.

4. Conclusions

In summary, we have demonstrated the preparation of CDs/PEG/CS composite. The tribology results showed that textured surfaces had good lubrication effect, and the texture-stored CDs/PEG/CS gel had slow-release effect that could effectively prolong the service life of artificial joints. Furthermore, the CDs/PEG/CS gel released rapidly under the rotation speed of 500–4000. CDs associated with PEG *via* hydrogen bond may be the primary factor causing the good lubrication effect.

Acknowledgements

This work is supported by National Natural Science Foundation of China (No. 51475358).

References

1 J. Bruce and R. Walmsley, *Br. J. Surg.*, 1937, **25**, 17–28.
2 S. M. Kurtz, O. K. Muratoglu, M. Evans and A. A. Edidin, *Biomaterials*, 1999, **20**, 1659–1688.
3 Y. L. Deng and D. S. Xiong, *J. Polym. Res.*, 2015, **22**, 195.
4 S. K. Gupta, A. Chu, A. S. Ranawat, J. Slamin and C. S. Ranawat, *J. Arthroplasty*, 2007, **22**, 787–799.
5 J. J. Jacobs, K. A. Roebuck, M. Archibeck, N. J. Hallab and T. T. Glant, *Clin. Orthop. Relat. Res.*, 2001, 71–77.
6 O. K. Muratoglu, K. Wannomae, S. Christensen, H. E. Rubash and W. H. Harris, *Clin. Orthop. Relat. Res.*, 2005, 158–164.
7 S. Watson, M. Nie, L. Wang and K. Stokes, *RSC Adv.*, 2015, **5**, 89698–89730.
8 M. Kobayashi and H. S. Hyu, *Materials*, 2010, **3**, 2753–2771.
9 E. C. A. Gee, R. Jordan, J. A. Hunt and A. Saithna, *J. Mater. Chem. B*, 2016, **4**, 1020–1034.
10 M. N. Collins, E. Dalton, J. J. Leahy and C. Birkinshaw, *RSC Adv.*, 2013, **3**, 1995–2007.
11 Y. Jiang, T. Jia, P. H. Wooley and S.-Y. Yang, *Acta Orthop. Belg.*, 2013, **79**, 1–9.
12 T. Moro, H. Kawaguchi, K. Ishihara, M. Kyomoto, T. Karita, H. Ito, K. Nakamura and Y. Takatori, *Biomaterials*, 2009, **30**, 2995–3001.
13 M. Kyomoto, T. Moro, Y. Takatori, S. Tanaka and K. Ishihara, *Clin. Orthop. Relat. Res.*, 2015, **473**, 942–951.
14 T. Moro, Y. Takatori, K. Ishihara, T. Konno, Y. Takigawa, T. Matsushita, U. I. Chung, K. Nakamura and H. Kawaguchi, *Nat. Mater.*, 2004, **3**, 829–836.
15 P. Bracco and E. Oral, *Clin. Orthop. Relat. Res.*, 2011, **469**, 2286–2293.
16 H. Zhang and S. H. Neau, *Biomaterials*, 2002, **23**, 2761–2766.
17 O. Jeon, R. Marks, D. Wolfson and E. Alsberg, *J. Mater. Chem. B*, 2016, **4**, 3526–3533.
18 M. Zhang, J. Liu, Y. Kuang, Q. Li, H. Chen, H. Ye, L. Guo, Y. Xu, X. Chen, C. Li and B. Jiang, *J. Mater. Chem. B*, 2016, **4**, 3387–3397.
19 V. X. Truong, M. L. Hun, F. Li, A. P. Chidgey and J. S. Forsythe, *Biomater. Sci.*, 2016, **4**, 1123–1131.
20 J. Kim, Y. P. Kong, S. M. Niedzielski, R. K. Singh, A. J. Putnam and A. Shikanov, *Soft Matter*, 2016, **12**, 2076–2085.
21 J. H. Seo, Y. Tsutsumi, A. Kobari, M. Shimojo, T. Hanawa and N. Yui, *Soft Matter*, 2015, **11**, 936–942.
22 W. F. Zhang, H. Zhu, S. F. Yu and H. Y. Yang, *Adv. Mater.*, 2012, **24**, 2263–2267.
23 X. Y. Xu, R. Ray, Y. L. Gu, H. J. Ploehn, L. Gearheart, K. Raker and W. A. Scrivens, *J. Am. Chem. Soc.*, 2004, **126**, 12736–12737.
24 B. G. Wang, W. W. Tang, H. S. Lu and Z. Y. Huang, *J. Mater. Chem. A*, 2016, **4**, 7257–7265.
25 H. Huang, H. Hu, S. Qiao, L. Bai, M. Han, Y. Liu and Z. Kang, *Nanoscale*, 2015, **7**, 11321–11327.
26 S. N. Baker and G. A. Baker, *Angew. Chem., Int. Ed.*, 2010, **49**, 6726–6744.
27 J. P. Gong, *Soft Matter*, 2006, **2**, 544–552.
28 C. W. McCutchen, *Wear*, 1962, **5**, 1–17.
29 H. Lu, W. Wang and A. Wang, *RSC Adv.*, 2015, **5**, 17775–17781.
30 M. Zhang, P. Yuan, N. Zhou, Y. Su, M. Shao and C. Chi, *RSC Adv.*, 2017, **7**, 9347–9356.
31 S. Wang, H. Niu, S. He and Y. Cai, *RSC Adv.*, 2016, **6**, 107717–107722.
32 J. Song, J. Li, Z. Guo, W. Liu, Q. Ma, F. Feng and C. Dong, *RSC Adv.*, 2017, **7**, 12827–12834.
33 L. G. Qin, P. Lin, Y. L. Zhang, G. N. Dong and Q. F. Zeng, *Appl. Surf. Sci.*, 2013, **268**, 79–86.
34 L. Qin, Q. Zeng, W. Wang, Y. Zhang and G. Dong, *J. Mater. Sci.*, 2014, **49**, 2662–2671.
35 B. X. Zhang, G. Y. Zhang, H. Gao, S. H. Wu, J. H. Chen and X. L. Li, *RSC Adv.*, 2015, **5**, 7395–7400.
36 P. Russo, A. Hu, G. Compagnini, W. W. Duley and N. Y. Zhou, *Nanoscale*, 2014, **6**, 2381–2389.
37 H. Gao, L. Song, W. Guo, L. Huang, D. Yang, F. Wang, Y. Zuo, X. Fan, Z. Liu, W. Gao, R. Vajtai, K. Hackenberg and P. M. Ajayan, *Carbon*, 2012, **50**, 4476–4482.
38 Y. Chen, J. Wang, H. Liu, M. N. Banis, R. Li, X. Sun, T.-K. Sham, S. Ye and S. Knights, *J. Phys. Chem. C*, 2011, **115**, 3769–3776.
39 Y. Li, Y. Zhao, H. Cheng, Y. Hu, G. Shi, L. Dai and L. Qu, *J. Am. Chem. Soc.*, 2012, **134**, 15–18.
40 Q. Liu, B. Guo, Z. Rao, B. Zhang and J. R. Gong, *Nano Lett.*, 2013, **13**, 2436–2441.
41 R. J. J. Jansen and H. Vanbekkum, *Carbon*, 1995, **33**, 1021–1027.
42 W. Wang, X. Yang, Y. Fang, J. Ding and J. Yan, *Appl. Energy*, 2009, **86**, 1196–1200.
43 M. A. Hussein, B. M. Abu-Zied and A. M. Asiri, *Polym. Compos.*, 2014, **35**, 1160–1168.
44 B. M. Abu-Zied, M. A. Hussein and A. M. Asiri, *Int. J. Electrochem. Sci.*, 2015, **10**, 1372–1383.
45 W. S. Zou, Y. J. Ji, X. F. Wang, Q. C. Zhao, J. Zhang, Q. Shao, J. Liu, F. Wang and Y. Q. Wang, *Chem. Eng. J.*, 2016, **294**, 323–332.
46 M. Wulff, M. Alden and D. Q. M. Craig, *Int. J. Pharm.*, 1996, **142**, 189–198.
47 T. Ozeki, H. Yuasa and Y. Kanaya, *Int. J. Pharm.*, 1997, **155**, 209–217.
48 D. M. Schachter, J. C. Xiong and G. C. Tirol, *Int. J. Pharm.*, 2004, **281**, 89–101.
49 M. N. Hyder and P. Chen, *J. Membr. Sci.*, 2009, **340**, 171–180.
50 A. B. Bourlinos, A. Stassinopoulos, D. Anglos, R. Zboril, M. Karakassides and E. P. Giannelis, *Small*, 2008, **4**, 455–458.